Appendix S1: Model formulation and parameter estimation details

A. Model formulation. We developed the Ecosystem-Disease (ED) model to describe infection in a primary producer and feedbacks through both disease and ecosystem characteristics. While there are a variety of modeling approaches that incorporate coupled elemental cycles via organismal physiology (Rastetter 2011), we chose to use a Droop model formulation (Droop 1973) to allow for a flexible stoichiometric balance in the uptake and decomposition of carbon and nutrients. With this formulation, the uptake rate of one resource varies with the availability of the others and is constrained to match the requirements of the organism. In the current analysis, we use a forest ecosystem as our case study because of the existence of a well-studied analogous model (Multiple-Element-Limitation) intended to describe a deciduous forest ecosystem (Rastetter & Shaver 1992; Rastetter *et al.* 1997). The ED modeling approach represents a simpler alternative (e.g., no threshold functions) and includes fewer parameters than the MEL model approach (Rastetter & Shaver 1992; Rastetter *et al.* 1997) but yields similar equilibrium predictions (Appendix Table S2). By reducing the number of parameters necessary to describe healthy forest ecosystem dynamics, we are able to expand the model (nearly doubling the parameters) to track both susceptible and infected vegetation. Because the ED model structure differed from (Rastetter *et al.* 1997), similar parameters took on new meaning and units. Additionally, forest ecosystem models do not include estimates for parameters associated with disease, so we estimated parameter values for the ED model from a variety of sources.

B. Parameter estimation. *Photosynthesis and death.* Growth rates via photosynthetic carbon capture for healthy vegetation of a deciduous hardwood forest have been estimated to be 585 g C m^{-2} y^{-1} (Fahey *et al.* 2005). Scaling this estimate to a forest stand (~12,000 g m^{-2}) yields 0.048 y^{-1}. We increased this estimate to parameterize a maximum growth rate ($\mu_S = 0.075$ y^{-1}), and then assumed that infection reduces maximum growth rate by up to 25% (e.g.,(Bloomberg & Morrison 1989)); while we explored the model sensitivity to this value, we assumed a 7% reduction for most of our simulations. We used the estimate for the death rate of healthy vegetation (δ_S=0.0412 y^{-1}) as the sum of vegetative litter production for C and respiration from (Rastetter *et al.* 1997). While there was no estimate of the death rate of infected vegetation for these forests ($\delta_I = 1.001 * \delta_S$), we assumed that this parameter was slightly higher because, while leaves may be lost substantially faster on average than in healthy trees, woody tissue will likely be lost only slightly faster.

Nutrient relations of vegetation. Growth occurs in the ED model as a function of the "cell quota" or the amount of nutrient (nitrogen) per unit of biomass (carbon) in the vegetation. We estimated the minimum cell quota for healthy trees ($q_s = 439^{-1}$) as the N:C ratio of wood as used by Rastetter 1997. While we had no data on the response of cell quota to nutrient availability in the ecosystem, because of flexible uptake and storage of nitrogen in trees (Lawrence 2001; Millard & Grelet 2010), we allowed more than a tripling for the maximum cell quota ($\widehat{Q_s} = 120^{-1}$) in response to N inputs, since we see substantial responses across taxa in (Bracken *et al.* 2014). To estimate the minimum cell quota for infected trees ($q_I = 438.7^{-1}$), we assumed that infected tissues have slightly higher N content than uninfected, because pathogens generally have lower C:N than their plant hosts (e.g., (LeROY *et al.* 2011; Grimmett *et al.* 2012)). Further, we assumed that if infection changed the maximum cell quota, it would increase N (e.g., (Grimmett *et al.* 2012)), so we estimated that this value ($\widehat{Q_I}$) would be 25% higher than

($\widehat{Q_S}$). The nutrient uptake rate of a deciduous forest has substantial uncertainty, but has been estimated as 31-171 kg N ha^{-1} y^{-1} (Groffman 2020) from which we estimated the specific nutrient uptake rate (N:C, c_S) as a function of carbon at the scale of a forest stand (~12,000 g m^{-2}) (Fahey *et al.* 2005) to obtain the range 0.00025 – 0.0059; we used an intermediate value, c_S =0.00038, in our simulations. As with our estimate of cell quotas, we assumed that the specific nutrient uptake rate for infected vegetation ($c_I = 1.001 * c_S$) was slightly higher. The ED model formulation required an estimate of the half saturation constant for nutrient uptake, which we were able to estimate based on a review of half saturation constants (~0.003 N m^{-2}) that included estimates for plant nutrient uptake (Mulder & Hendriks 2014). We assumed that this was the same for both healthy (a_S) and infected vegetation (a_I).

Environmental carbon and nutrients. We parameterized this model with carbon and nitrogen, primarily because these were the elements for which most empirical data were available. While many ecosystems on Earth are being modified by significant anthropogenic nitrogen inputs (Galloway *et al.* 2004), and the model can be modified to include inputs and outputs of nitrogen, for the current modeling exercise, we model this as a closed system with no losses or gains of nitrogen. In contrast, we model carbon as being taken up at a rate modified by the nutrient relations of the vegetation ($\mu_i(Q_i)$, for $i = S, I$). Estimates of carbon loss rates (ϵ_S) from natural system to e.g., CO_2, dissolved organic carbon, or recalcitrant forms vary. While Rastetter 1997 assumed this parameter was zero, estimates of decomposition rates of branches and litterfall range from .145 to .58 y^{-1} (Fahey *et al.* 2005). We used a value intermediate to these estimates, $\epsilon_S = 0.0648$ per year. Because pathogen infection can slow decomposition of some deciduous hardwood leaves (Grimmett *et al.* 2012), we assume that carbon loss from infected vegetation ($\epsilon_I = 1.1 * \epsilon_S$) is slightly higher than healthy vegetation. The annual rate of net nitrogen mineralization was estimated from two values. Forest nitrogen estimates from Hubbard Brook range from 626 g m^{-2} to 820 g m^{-2} (Yanai *et al.* 2013), and net nitrogen mineralization rates range from 3.1 to 17.1 g m^{-2} y^{-1} (Groffman 2020). The per year rate estimate from the quotient of these ranges from 0.0038 to 0.027, and we used a parameter value that falls between these (r=0.0084).

Transmission rates. We assume that transmission depends on the N:C of infected hosts with a saturating Michaelis Menten form with maximum transmission rate $\hat{\beta}$ and half saturation constant κ. In order to parameterize the maximum transmission rate $\hat{\beta}$, we considered a simplified SI model of susceptible and infected vegetation with biomass in terms of g C m^{-2} with a constant total population density of S+I=N=12,006 g C m^{-2} (Fahey *et al.* 2005):

$$S'(t) = -\hat{\beta}SI, I'(t) = \hat{\beta}SI.$$

Solving this system yields an expression for $\hat{\beta} = \frac{1}{Nt}\ln\left(\frac{S(0)(N-S(t))}{S(t)(N-S(0))}\right)$.

We assumed initial conditions with one infected tree with bark disease (e.g. beech bark disease, Dutch elm disease), where 6.4% of the tree's C is bark (Fahey *et al.* 2005), and all of the bark is infected. Here, we assume a tree has 7 million grams of carbon total thus resulting in $4.28 * 10^{-5}$ g C of bark. Empirical estimates of rates of spread of diseases across North American forests range from 4.2 to 57 km/year (Evans 2016). We consider these two extreme rates of spread to estimate a range for $\hat{\beta}$. First consider a forest with area 4200 m^2 and assume the initially infected population is $4.28 * 10^{-5}$ g C/4200

m^2. For the second case, we consider a forest with area 57000 m^2 and an initially infected population is $4.28 * 10^{-5}$ g C/57000 m^2. Considering ranges that yield in 15-50% of the bark per meter squared becoming infected after one year results in a range of $\hat{\beta}$ from $6.5 * 10^{-6}$ to $3.3 * 10^{-4}$. The simulations throughout the manuscript use the value $\hat{\beta} = 1.2 * 10^{-5}$. We considered empirical measurements of nitrogen induced changes in spore production of barley fungal pathogens (Jensen and Munk 1997) to parameterize the half saturation constant κ. Jensen and Munk 1997 varied N supply from 30-240 mg N per pot on seedlings of spring barley inoculated with powdery mildew and observed variations in spore productions. Estimating the half saturation to occur between 70 and 120 mg N per pot and considering their pots had surface area of 182 cm^2 yields a range of 3.8 - 6.5 g N m^{-2}. Assuming a forest stand size of (~12,000 g C m^{-2}) (Fahey *et al.* 2005) with the assumption that only 5-10% of this C produces spores yields a possible range for κ of 0.003 – 0.01 g N per g C. We used $\kappa = 0.009$ throughout the simulations.

Aligning with earlier work. After estimating parameter values from the empirical literature, we ran the ED model to estimate equilibria, then compared the equilibrium values we obtained to those generated by the MEL model parameterized for a deciduous forest (Rastetter *et al.* 1997). While empirical literature provided realistic ranges for each parameter, we sought to compare the dynamic influence of disease in an ecosystem. Therefore we chose values inside their respective ranges such that the ED model parameters, in the absence of infection, generated equilibrium solutions that closely matched (Rastetter *et al.* 1997) (see Table 2 for parameter values). Thus, while the ED model structure differs, the steady state values (in the absence of disease) closely resemble those of a well-known forest ecosystem model (Rastetter *et al.* 1997) (Appendix Table S1).

Appendix Table S1. Comparison of steady states from the forest model of (Rastetter *et al.* 1997) with the steady states of the current model using the parameters from Table 1 (main text), demonstrating that the values in the ED uninfected forest model is quantitatively comparable to this earlier work.

	Plant C (kg C m^{-2})	Plant N (g N m^{-2})	Soil Organic C (kg C m^{-2})	Soil Organic N (g N m^{-2})	Plant C:N (g C : g N)	Soil Inorganic N (g N m^{-2})
Rastetter et al. with doubled $C0_2$	22.57	111.3	13.24	519.90	202.80	0.78
Rastetter et al. without doubling $C0_2$	22.00	110.00	13.00	520.99	200.00	0.88
ED model (no disease)	21.31	107.02	13.51	524.13	199.12	0.84

C. Parameter sensitivity. While all parameter values were taken from empirical literature and disease-free model results were comparable to previous modeling efforts, we note the significance of the ED model predictions are largely qualitative rather than quantitative. Indeed, equilibria predictions are sensitive to variations in parameters (Figs. 4 and 5). Transient dynamics are also sensitive to variations in parameters (not shown). The ED model formulation and parameterization efforts provide a starting

point that highlights the impact of coupling ecosystem with disease dynamics; however, thorough parameter sensitivity analyses should be conducted before using this model for quantitative predictions. Appendix S5 provides a global parameter analysis for the case study of the model parameterized for this forest ecosystem.

Appendix S2: Model implementation and simulations

A. Model simulations were performed using MATLAB and the built in ordinary differential equation solvers, ode45 and ode23s. Initial conditions were taken to match initial conditions and equilibrium scenarios used in (Rastetter *et al.* 1997) with a small initial amount of infected vegetation; $S_0 = 2200, I_0 = 0.0005, D_{S_0} = 1300\ D_{I_0} = 0, R_{S_0} = 521, Q_{S_0} = 190^{-1}, Q_{I_0} = 190^{-1}, N_0 = 1$. Simulations of the model without disease assigns a zero infected population, $I_0 = 0$.

B. Initial amount of infected carbon. With the current parameterization to describe a 250-year old deciduous forest, the duration of the ED model's transient dynamics was fairly insensitive to the initial amount of infected vegetation carbon. For example, with a 1000-fold increase in the initial amount of vegetation carbon that is infected ($I_0 = 0.5$) compared to the initial infection value assumed in the main text, the transient dynamics still last for 200 years, compared to the 300 year duration of transient dynamics produced when the value of initial infected vegetation carbon is 0.0005 (value assumed in the main text; Appendix Fig. S1).

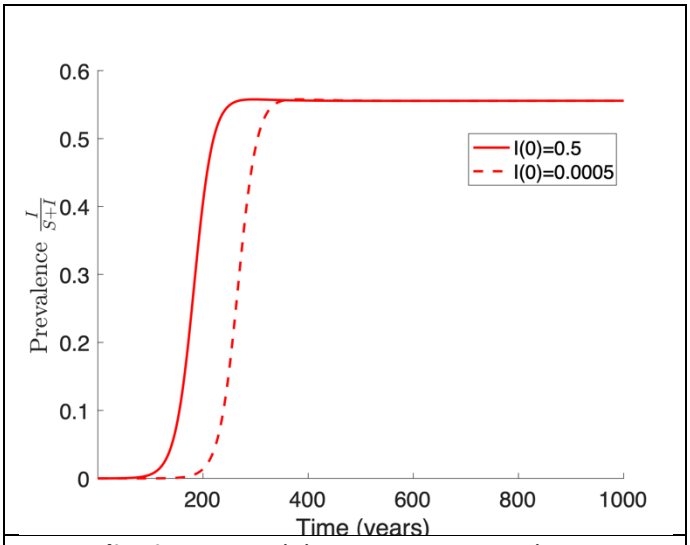

Appendix Fig. S1. Model sensitivity to initial amount of infected carbon.

C. Simulating scenarios with no feedback. Simulations to mimic more traditional SI modeling that do not account for ecosystem dynamics and feedbacks (Fig. 3, main text) assumed that the C:N ratios of the vegetation are constant. This was implemented by assigning a single invariant value for C:N. These equations are shown in Appendix Table S2. We simulated two scenarios, one with equal stoichiometric ratios for susceptible and infected ($Q_S = Q_I = 190^{-1}$; results not shown) and another with different values for susceptible and infected, assigned based on the equilibrium values ($Q_S = 200^{-1}, Q_I = 180^{-1}$; Fig. 3).

D. Impact of the range of predicted transmission values. To explore the impact of the range of variation in transmission (due to dependence on nutrient feedbacks) shown in Fig. 3c, we ran simulations at several different values for infected vegetation C:N ratio, while assuming vegetation C:N was constant within a simulation, and observed its influence on disease prevalence (black lines in Fig. 3d). Infected vegetation C:N ratios from $Q_I \in (179.5^{-1}, 188^{-1})$ correspond to transmission rates of the range $\beta(Q_I) \in (4.46 - 4.58) * 10^{-6}$). For these simulations, we also fixed the healthy vegetation C:N ratios to be equal to those of the infected vegetation, i.e. $Q_S = Q_I$. The blue lines in Fig. 3d consider scenarios

Appendix Table S2. Model equations for uncoupled model in Fig. 3, main text.

$$\frac{dS}{dt} = \underbrace{\mu_S(Q_S)S + \mu_I(Q_I)I}_{growth} - \underbrace{\beta(Q_I)SI}_{infection} - \underbrace{\delta_S S}_{death}$$

$$\frac{dI}{dt} = \underbrace{\beta(Q_I)SI}_{infection} - \underbrace{\delta_I I}_{death}$$

$$\frac{dD_S}{dt} = \underbrace{\delta_S S}_{death\ released\ C} - \underbrace{\epsilon_S D_S}_{C\ loss}$$

$$\frac{dD_I}{dt} = \underbrace{\delta_I I}_{death\ released\ C} - \underbrace{\epsilon_I D_I}_{C\ loss}$$

$$\frac{dR_S}{dt} = \underbrace{\delta_S S Q_S}_{death\ released\ N} - \underbrace{rR_S}_{N\ recycling}$$

$$\frac{dR_I}{dt} = \underbrace{\delta_I I Q_I}_{death\ released\ N} - \underbrace{rR_I}_{N\ recycling}$$

$$\frac{dQ_S}{dt} = 0$$

$$\frac{dQ_I}{dt} = 0$$

$$\frac{dN}{dt} = 0$$

Where

$\mu_i(Q_i) = \hat{\mu_i}\left[1 - \frac{q_i}{Q_i}\right]$ (For Blue lines in Fig. 3d $\mu_i = 0.0401$ held constant)

$\beta(Q_I) = \frac{\hat{\beta} Q_I}{\kappa + Q_I}$

without any elemental feedbacks. Here, vegetation C:N ratios are fixed ($Q_S = Q_I = 190^{-1}$) but transmission is varied within the same range through slight variations in $\hat{\beta}$. In both scenarios, $\beta = 4.42 * 10^{-6}$ is denoted by dotted curves, $\beta = 4.49 * 10^{-6}$ dashed curves, and, $\beta = 4.56 * 10^{-6}$ solid curves.

E. Long transient dynamics. Figs 4 and 5 in the main text show equilibrium solutions of the model as parameters vary. Because transient dynamics for some components of the model were extremely long, except where noted, the values shown in graphs are the solutions to the model at 10,000 years.

F. Impact of total system nitrogen. Fig. 5 varies the total amount of nitrogen in the system. The model assumes the system is closed for nitrogen. To examine the effect of total ecosystem nitrogen on disease and ecosystem variables, we vary the total amount of nitrogen and track the pools in soil and vegetation. The initial conditions used in a multiple element forest ecosystem model (Rastetter *et al.* 1997) assumed the nitrogen was distributed across the systems such that 0.1% of the total nitrogen in the forest was in the form of soil inorganic N, 81.7% was preset as soil organic C, and 18.2% was contained in live vegetation. To remain comparable to the earlier work, we assigned these proportions for initial conditions as we varied the total amount of nitrogen.

Appendix S3: Virulence effects on equilibria

We investigated how the dynamics of the system change to variations in virulence, where virulence is the percent reduction in the maximum growth rate of infected hosts vs susceptible hosts. The model solutions approach an equilibrium value, but although the stability of this equilibrium appears robust to changes in virulence, the value of the equilibrium changes. Furthermore, for small variations in virulence (6.85-7.1%) we see significant changes in the equilibrium value (Appendix Fig. S2) that appear to be robust to variations in initial conditions (not shown). Life history traits (e.g. growth rates) also were identified as important parameters in a full parameter sensitivity analysis for the forest system case study (Appendix S5).

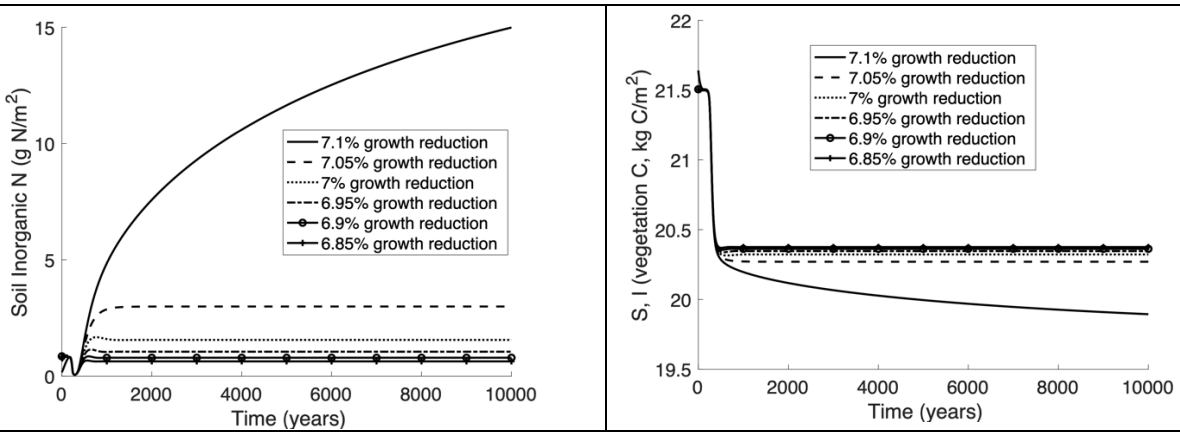

Appendix Fig. S2. Model sensitivity to variations in virulence.

Appendix S4: Elasticity Index of the Basic Reproductive Number

The expression for the basic reproductive number is:

$$R_0 = \frac{\beta(Q_i^*)S^*}{\delta_I} = \frac{\hat{\beta}Q_I^*S^*}{(\kappa + Q_I^*)\delta_I}.$$

This clearly depends on the susceptible host population size at the disease-free equilibrium (S^*) as well as transmission rate, which is a function of the infected N:C ratio at the disease-free equilibrium, Q_I^*. Both of these disease-free equilibrium values depend on N supply. Varying total N in the system, we see a critical value of total N where R_0 becomes greater than one. The disease cannot persist if N is below this critical threshold. In Figure 5a of the main text, two different terms of the expression for R_0 are plotted separately, $\beta(Q_I^*)/\delta_I$ and S^* to see the relative impact of these two terms. We scaled the values by a factor of 10,000 for easier visualization. It is clear from the steep slope of S^*, that the population size is a dominant factor when disease dynamics are driven by total N. Below, we further explore these factors with elasticity indexes.

Normalized sensitivity indexes, called elasticity indexes of R_0, are useful measures of the relative importance of different factors responsible for transmission (van den Driessche 2017). The elasticity index of R_0 with respect to S^* is defined as

$$\Upsilon_{S^*}^{R_0} = \frac{\partial R_0}{\partial S^*} \times \frac{S^*}{R_0} = 1$$

and the elasticity index of R_0 with respect to Q_I is defined as

$$\Upsilon_{Q_I}^{R_0} = \frac{\partial R_0}{\partial Q_I} \times \frac{Q_I}{R_0} = \frac{\beta'(Q_I)}{\beta(Q_I)} Q_I.$$

The assumptions built into this model, where $\beta(Q_I)$ is an increasing, saturating function of the form $\beta(Q_I) = \frac{\widehat{\beta} Q_I}{\kappa + Q_I}$ result in an elasticity index $\Upsilon_{Q_I}^{R_0} = \frac{\kappa}{\kappa + Q_I}$ which is plotted in Appendix Fig. S3 as total N varies. Here, $\Upsilon_{Q_I}^{R_0}$ increases slightly as Total N increases, but is always less than $\Upsilon_{S^*}^{R_0} = 1$. It is important to note that the slope and magnitude of this elasticity index for Q_I depend on the transmission function β. While, these variations in the elasticity of R_0 with respect to Q_I appear small for this parameterization of our model, we note it may play a bigger role under different conditions when the model is parameterized for different types of ecosystems.

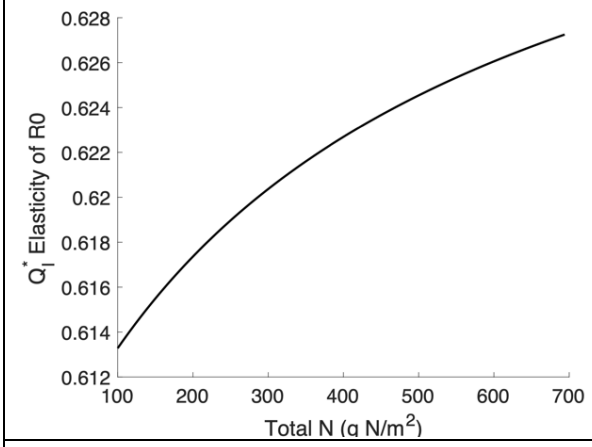

Appendix Fig. S3. The slope and magnitude of the elasticity index of R_0 with increasing total N in the system.

Appendix S5: Parameter Sensitivity Analyses

We performed a global parameter sensitivity analysis for the model as parameterized for a forest ecosystem using Latin Hypercube Sampling (LHS) with the statistical Partial Rank Correlation Coefficient (PRCC) technique. LHS is a stratified Monte Carlo sampling method without replacement giving an unbiased selection of parameter values. To assess the relative importance of each parameter, PRCC offers a statistical technique that is appropriate when the parameters have a monotonic relationship with the output measures (Marino *et al.* 2008). We considered 1) live host carbon density, 2) infection prevalence, and 3) soil inorganic N levels after 10,000 years as output measures and explored parameter ranges given in Appendix Table S3 with 5,000 LHS samples. We calculated the PRCC values (Appendix Fig. S4) since the majority of these parameter values had monotonic relationships with the output measures (Appendix Fig. S5).

a. PRCC values for live host density

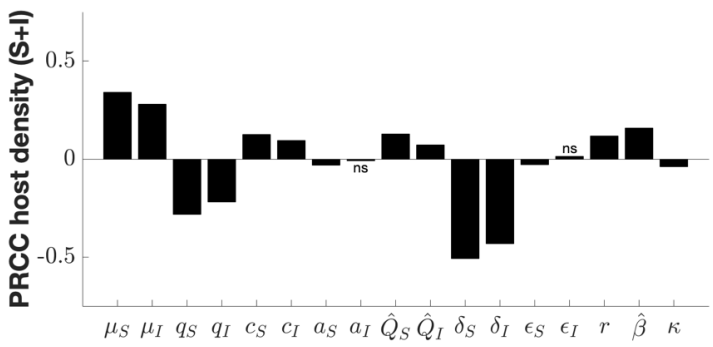

The only non-monotonic relationship was between δi and soil inorganic N, where we investigated the sensitivity in truncated monotonic ranges and obtained similar results, following the method described in Gomero (Gomero 2012).

In general, for a given parameter the higher the PRCC value is in magnitude the more influential that parameter is to the output measure. A positive PRCC value means an increase in that parameter results in an increase in the output measure, whereas an increase in a parameter with a negative PRCC values yields a decrease in the output measure. Following Marino *et al.* (Marino *et al.* 2008) we performed a z-test on the resulting PRCC values and verified that, in general, higher magnitude PRCC values corresponded with a stronger influence on the output measure.

b. PRCC values for prevalence

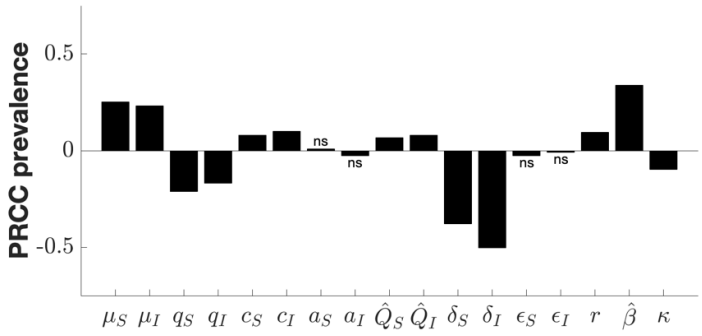

c. PRCC values for soil inorganic N

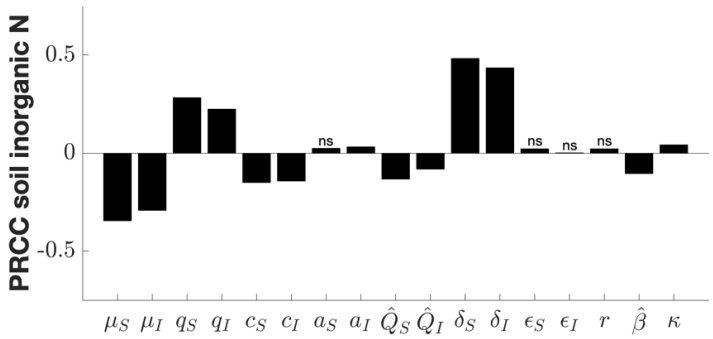

Appendix Fig. S4. Parameter sensitivity analysis results for Latin Hypercube Sampling (5,000 samples), parameter ranges and baseline values given in Appendix Table S3, for above output measures at 10,000 years. PRCC values marked as ns are not significant (P>0.05).

Our parameter sensitivity analysis identified life-history traits (maximum growth rates and death rates) as well as stoichiometric traits (minimum N:C ratios) as important parameters across all three output measures. Infection prevalence was also sensitive to the maximum transmission rate.

[Appendix Fig. S5 on next page]

a. Monotonicity plots for live host density

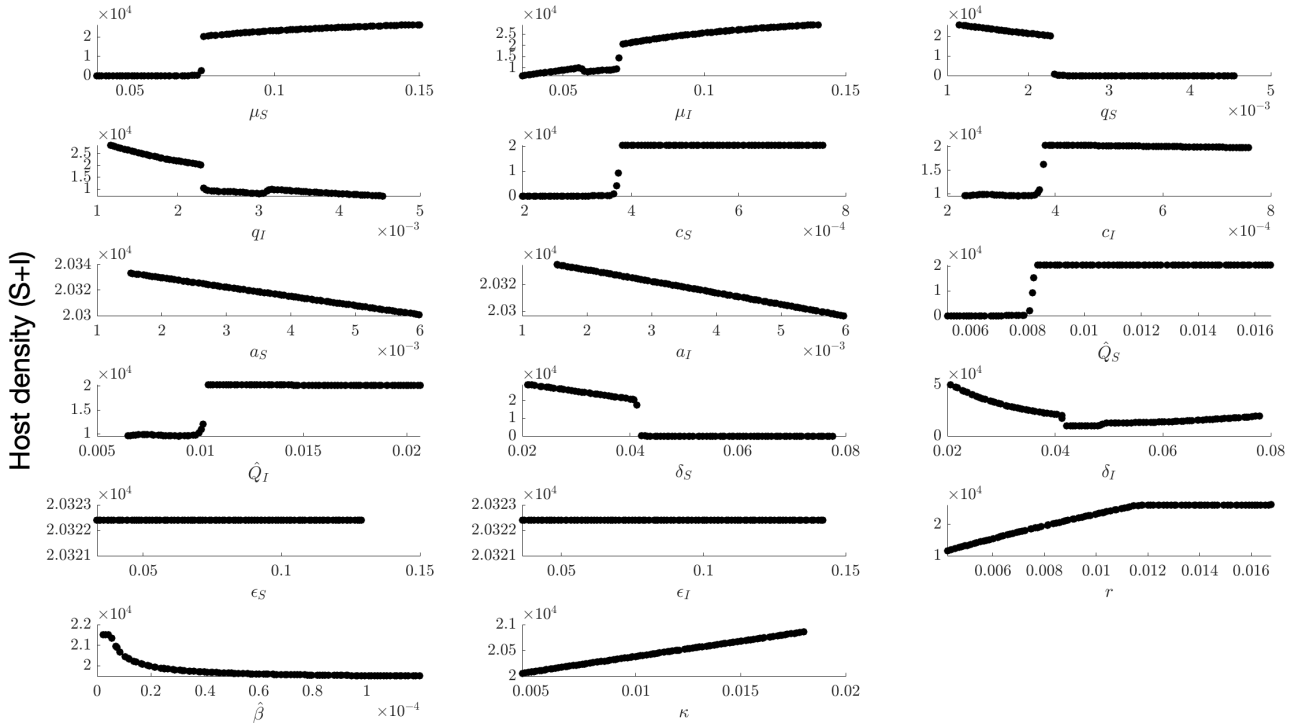

b. Monotonicity plots for prevalence

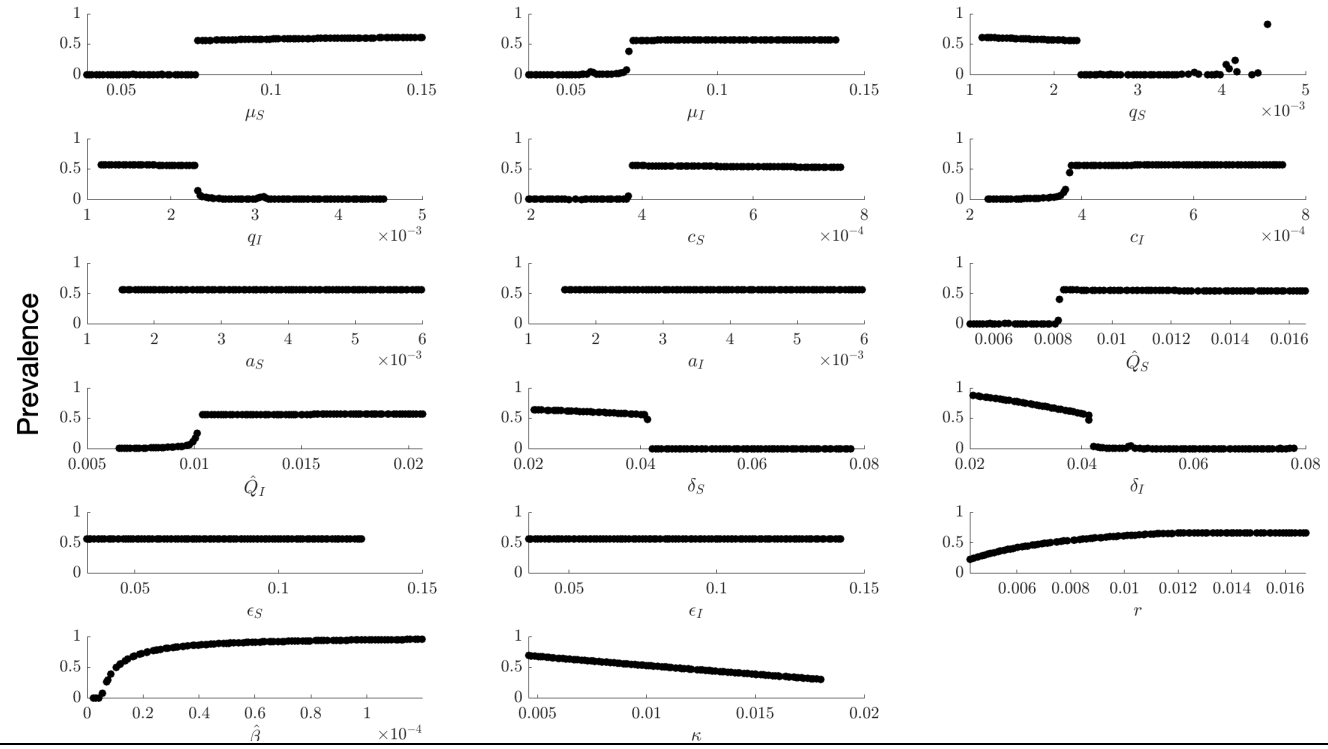

c. Monotonicity plots for soil inorganic N

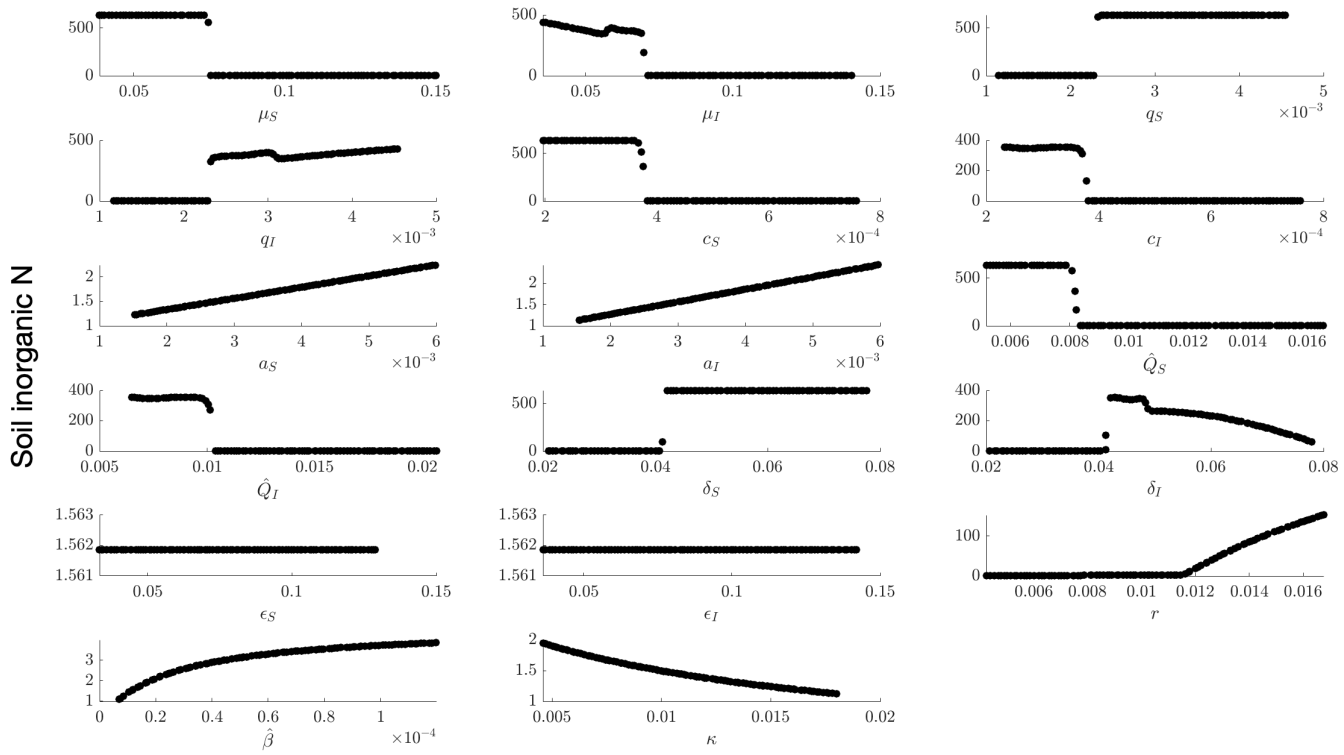

Appendix Fig. S5. Monotonic relationships between parameters values and three different key output measures. Plots show the variation of a single parameter at a time while all other parameters were held constant at the baseline values in Appendix Table S3.

Supplemental Information References Cited

1.

Bloomberg, W.J. & Morrison, D.J. (1989). Relationship of growth reduction in Douglas-fir to infection by Armillaria root disease in southeastern British Columbia. *Phytopathology*, 79, 482-487.

2.

Bracken, M.E.S., Hillebrand, H., Borer, E.T., Seabloom, E.W., Cebrian, J., Cleland, E.E. *et al.* (2014). Signatures of nutrient limitation and co-limitation: responses of autotroph internal nutrient concentrations to nitrogen and phosphorus additions. *Oikos*, n/a-n/a.

3.

Droop, M.R. (1973). Some thoughts on nutrient limitation in algae. *Journal of Phycology*, 9, 264-272.

4.

Fahey, T.J., Siccama, T.G., Driscoll, C.T., Likens, G.E., Campbell, J., Johnson, C.E. *et al.* (2005). The Biogeochemistry of Carbon at Hubbard Brook. *Biogeochemistry*, 75, 109-176.

5.

Galloway, J.N., Dentener, F.J., Capone, D.G., Boyer, E.W., Howarth, R.W., Seitzinger, S.P. *et al.* (2004). Nitrogen cycles: past, present, and future. *Biogeochemistry*, 70, 153-226.

6.

Gomero, B. (2012). Latin Hypercube Sampling and Partial Rank Correlation Coefficient Analysis Applied to an Optimal Control Problem.

7.

Grimmett, I.J., Smith, K.A. & Bärlocher, F. (2012). Tar-spot infection delays fungal colonization and decomposition of maple leaves. *Freshwater Science*, 31, 1088-1095.

8.

Groffman, P.M. (2020). Chapter 07: Nitrogen Cycling. In: *Online Book: A Synthesis of Scientific Research at Hubbard Brook* (eds. Likens, GE & Groffman, PM) Hubbard Brook.

9.

Lawrence, D. (2001). Nitrogen and phosphorus enhance growth and luxury consumption of four secondary forest tree species in Borneo. *Journal of Tropical Ecology*, 17, 859-869.

10.

LeROY, C.J., FISCHER, D.G., HALSTEAD, K., PRYOR, M., BAILEY, J.K. & SCHWEITZER, J.A. (2011). A fungal endophyte slows litter decomposition in streams. *Freshwater Biology*, 56, 1426-1433.

11.

Marino, S., Hogue, I.B., Ray, C.J. & Kirschner, D.E. (2008). A methodology for performing global uncertainty and sensitivity analysis in systems biology. *Journal of theoretical biology*, 254, 178-196.

12.

Millard, P. & Grelet, G.-a. (2010). Nitrogen storage and remobilization by trees: ecophysiological relevance in a changing world. *Tree Physiology*, 30, 1083-1095.

13.

Mulder, C. & Hendriks, A.J. (2014). Half-saturation constants in functional responses. *Global Ecology and Conservation*, 2, 161-169.

14.

Rastetter, E.B. (2011). Modeling coupled biogeochemical cycles. *Frontiers in Ecology and the Environment*, 9, 68-73.

15.

Rastetter, E.B., Agren, G.I. & Shaver, G.R. (1997). Responses of N-Limited Ecosystems to Increased CO$_2$: A Balanced-Nutrition, Coupled-Element-Cycles Model. *Ecological Applications*, 7, 444-460.

16.

Rastetter, E.B. & Shaver, G.R. (1992). A Model of Multiple-Element Limitation for Acclimating Vegetation. *Ecology*, 73, 1157-1174.

17.

van den Driessche, P. (2017). Reproduction numbers of infectious disease models. *Infect Dis Model*, 2, 288-303.

18.

Yanai, R.D., Vadeboncoeur, M.A., Hamburg, S.P., Arthur, M.A., Fuss, C.B., Groffman, P.M. *et al.* (2013). From Missing Source to Missing Sink: Long-Term Changes in the Nitrogen Budget of a Northern Hardwood Forest. *Environmental Science & Technology*, 47, 11440-11448.